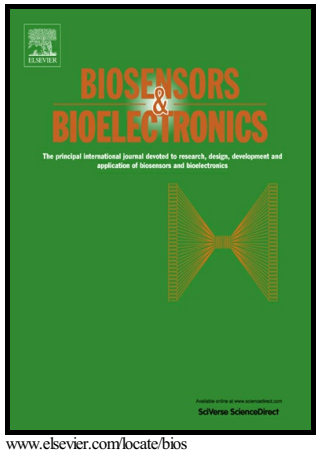

www.elsevier.com/locate/bios

Dual-signal amplified photoelectrochemical biosensor for detection of N^6-methyladenosine based on $BiVO_4$–110-TiO_2 heterojunction, Ag+-mediated cytosine pairs

Haiyan Wang, Huanshun Yin, Hua Huang, Kelin Li, Yunlei Zhou, Geoffrey I.N. Waterhouse, Hai Lin, Shiyun Ai

PII: S0956-5663(18)30157-X
DOI: https://doi.org/10.1016/j.bios.2018.02.056
Reference: BIOS10318

To appear in: *Biosensors and Bioelectronic*

Received date: 31 October 2017
Accepted date: 26 February 2018

Cite this article as: Haiyan Wang, Huanshun Yin, Hua Huang, Kelin Li, Yunlei Zhou, Geoffrey I.N. Waterhouse, Hai Lin and Shiyun Ai, Dual-signal amplified photoelectrochemical biosensor for detection of N^6-methyladenosine based on $BiVO_4$–110-TiO_2 heterojunction, Ag+-mediated cytosine pairs, *Biosensors and Bioelectronic,* https://doi.org/10.1016/j.bios.2018.02.056

Dual-signal amplified photoelectrochemical biosensor for detection of N^6-methyladenosine based on $BiVO_4$-110-TiO_2 heterojunction, Ag+-mediated cytosine pairs

Haiyan Wang [1], Huanshun Yin [1,*], Hua Huang [1], Kelin Li [2], Yunlei Zhou [1], Geoffrey I.N. Waterhouse [1,3], Hai Lin [2,*], Shiyun Ai [1]

[1] College of Chemistry and Material Science, Shandong Agricultural University, Tai'an 271018, P.R. China

[2] College of Animal Science, Shandong Agricultural University, Tai'an 271018, P.R. China

[3] School of Chemical Sciences, The University of Auckland, Private Bag 92019, Auckland, New Zealand

*Corresponding author.

E-mail: yinhs@sdau.edu.cn (Huanshun Yin), hailin@sdau.edu.cn (Hai Lin)

Abstract:

Herein, a novel dual-signal amplified photoelectrochemical (PEC) biosensor was successfully developed for the highly selective detection of N^6-methyladenosine (m^6A) methylated RNA. The PEC biosensor comprised $BiVO_4$-110-TiO_2 heterojunction and gold nanoparticle decorated MoS_2 (MoS_2-AuNPs) as the photoactive materials, horseradish peroxidase conjugated biotin (HRP-Biotin) as the enzymatic unit, Ag^+-mediated cytosine pairs (C-Ag^+-C) as the signal amplification unit, and the anti-m^6A antibody as the m^6A methylated RNA recognition unit. Following immunoreaction between m^6A and the anti-m^6A antibody, the C-Ag^+-C structure of the hairpin DNA unfolded, yielding the duplex strand DNA (dsDNA) and releasing Ag^+ ions. Superoxide ions (O_2^-) generated by the action of HRP on H_2O_2 then served as an electron donor, resulting in the deposition of Ag on AuNPs surface and resulting in an increased photocurrent. Based on this change f the photocurrent, m^6A could be accurately assayed using this dual-signal amplified PEC biosensor. The biosensor showed high selectivity and a very low detection limit of 1.665 pM for m^6A, and was successfully applied to evaluate the content change of m^6A in leaves of maize seedling and chicken fetal hepatocytes samples after treatment with chemical mutagen of ethylmethane sulfonate and hormone of insulin, respectively.

Keywords: Photoelectrochemical biosensor; N^6-methyladenosine; Gold nanoparticle decorated MoS_2; RNA methylation; chicken fetal hepatocyte; maize seedling leaves.

1. Introduction

RNA methylation plays a vital role in post-transcriptional regulation of gene expression in higher eukaryotes (He 2010). N^6-methyladenosine (m^6A) has been discovered as the first example of the reversible and dynamic

biosensor for kinase activity detection (Wang et al. 2017b). In our previous work, an improved PEC method was reported for the sensitive detection of protein kinase A activity using TiO_2/g-C_3N_4 (Li et al. 2017). Further, a simple PEC immunosensor was developed for detecting methylated RNA based on g-C_3N_4/CdS heterojunctions (Wang et al. 2017a). In PEC bioanalysis system, it is vital to select appropriate photoactive materials with high photocurrent conversion efficiencies (Zhang et al. 2017; Feng et al. 2017). This allows an enhanced PEC response and thus high sensitively towards a target molecule, thereby allowing detection of the target at low concentrations. Recently, monoclinic $BiVO_4$ with narrow bandgap energy of 2.4 eV and a strong visible light response has attracted great attention in the field of semiconductor phototocatalysis (Kudo et al. 1999). In addition to its narrow band gap, $BiVO_4$ has many other useful and interesting properties inlcuding its ferroelasticity, ionic conductivity, non-toxicity, long-term chemical stability and low cost (Li et al. 2014; Zhao et al. 2016). However, the photocatalytic performance of pristine $BiVO_4$ is limited because of fast electrons-hole pair recombination after photoexcitation, and poor electron transfer properties. In order to overcome these limitations, $BiVO_4$ is commonly coupled with other semiconductors to form heterojunctions (e.g. g-C_3N_4/$BiVO_4$ (Li et al. 2014), MoS_2/$BiVO_4$ (Li et al. 2015b), $BiVO_4$/WO_3 (Tateno et al. 2017), which significantly improves photocatalytic efficiencies by facilitating effective charge separation. Recently, $BiVO_4$-TiO_2 heterostructures have attracted great attention (Singh et al. 2016). However, Li et al. proposed that $BiVO_4$-TiO_2 heterojunctions with different $BiVO_4$ interfacial contact facets ({110} facet or {010}

facet) displayed different photocatalytic performance and the $BiVO_4$-110-TiO_2 heterojunctions ($BiVO_4$@TiO_2) were reported to afford high photocurrent densities and low photoluminescence intensities, suggesting their suitability for PEC biosensor development (Li et al. 2015a). To our knowledge, $BiVO_4$@TiO_2 has not previously been applied in the construction of a PEC biosensor for m^6A detection.

Layered MoS_2, a graphene-like two-dimensional semiconductor nanomaterial, possesses a bandgap of 1.2-1.9 eV deponding on its thickness. MoS_2 nanosheets exhibit excellent charge carrier mobility, and are considered as promising alternatives to TiO_2 and other conventional semiconductor materials in many technologically important areas (Xie et al. 2013). MoS_2 itself is generally incapable of immobilizing target molecules, except for the capture of nucleotides via van der Waals forces (Zhu et al. 2013). Thus, pure MoS_2 is difficult to use directly in PEC biosensors. However, MoS_2 is excellent semiconductor support that can stabilize noble metallic nanoparticles (such as Au, Ag, Pd, and Pt NPs) to form hierarchical nanocomposites (Huang et al. 2013). Accordingly, functionalisation of MoS_2 nanosheets with noble metallic nanoparticles is an excellent approach for extending the application range of the semiconductor (Huang et al. 2013). For example, MoS_2 sheets decorated with gold nanoparticles (MoS_2-AuNPs) demonstrate superior photocatalytic activity relative to pristine MoS_2 sheets (Yin et al. 2014). Further, AuNPs show good biocompatibility and electronic properties, and are now widely utilized in biosensors and as biomolecule labels (Zang et al. 2017). Semiconductor-supported bimetallic Ag-AuNPs demonstrate superior properties to Au NPs in terms of promoting rapid

transfer of photogenerated carriers and reducing recombination rates of electron-hole pairs (Baek et al. 2014; Zhang et al. 2016). To date, MoS_2-AuNPs or MoS_2-Ag-AuNPs nanocomposites have not yet been utilized in a PEC biosensor for m^6A assay.

Ag^+-mediated DNA pairs, where the hydrogen bonds between base pairs DNA are replaced by Ag^+-base bonds, are becoming more commonly used in analytical research and nanotechnology (Enkin et al. 2014; Ono et al. 2008). Cytosine-silver ion-cytosine (C-Ag^+-C) is a particularly stable type of Ag^+-mediated base pair. Researchers have demonstrated that the C-Ag^+-C structure is more stable than A-Ag^+-A and T-Ag^+-T, where A and T represent adenine and thymine, respectively. The binding energy (BE) of C-Ag^+-C was calculated be lower than that of the Watson-Crick (WC) base pairs, indicating that the addition of sufficient complementary base could reconfigure C-Ag^+-C pairs to more stable WC pairs (Swasey et al. 2015). This provided a key trigger for the development of a novel PEC biosensor for m^6A in mRNA.

Herein, we aimed to develop a sensitive PEC biosensor for m^6A in total RNA, that integrated the many advantages of $BiVO_4$@TiO_2 heterojunctions, MoS_2-AuNPs and C-Ag^+-C for PEC applications. Further, we sought to explore the applicability of the PEC biosensor, by investigating the expression level change of m^6A methylated RNA in the extracted totall RNA of the leaves of maize seedlings and chicken fetal hepatocyte, where the leaves of maize seedlings were obtained from maize seed treated with ethylmethane sulfonate (EMS) mutagenesis, and the chicken fetal

hepatocytes were treated with different contrations of insulin.

2. Experimental

2.1 Materials and reagents

The oligonucleotides used in this work and HRP-conjugated Avidin (Avidin-HRP) were obtained from Sangon Biotech (Shanghai) Co., Ltd. (China) and the base sequences are as follows. Probe DNA (hDNA), 5'-NH_2-GCG CGG GCC CCC AAA AAA AAA GCG GCC CCC CG-3'. Complementary DNA, 5'-Biotin-CG GGG GGC CGC TTT TTT TTT GGG GGC CCG CGC-3'. The other materials and buffer solutions are shown in supplementary material.

2.2 Synthesis of $BiVO_4$@TiO_2 heterojunctions, MoS_2-AuNPs nanohybrids and Avidin-SiO_2-hDNA@Ag

The preparation process of $BiVO_4$, $BiVO_4$@TiO_2 heterojunction and MoS_2-AuNPs nanohybrid was displayed in supplementary material.

The Avidin-SiO_2-hDNA@Ag composite was synthesized as follows. Firstly, SiO_2 nanoparticles with surface carboxy groups were synthesized according to previous paper (Zhang et al 2006). 1.77 mL TX-100, 7.5 mL cyclohexane, 1.8 mL 1-hexanol were firstly mixed with 340 μL double distilled deionized water. Then 100 μL TEOS and 60 μL NH_4OH (25%) were successively added into the above solution with stirring, and the stirring continued for 24 h. Subsequently, 50 mL of acetone was added and the sediment collected, washed with ethanol and doubly distilled deionized water (three times for the latter). After drying at 60 °C for 12 h, a white powder was obtained. The SiO_2 product was dispersed in 10 mM PBS (pH 7.4) for later use (the

SiO_2 concentration was 1 mg/mL).

Prior to the preparation of Avidin-SiO_2-hDNA@Ag, DNA strands were annealed to 90 °C for 5 minutes and cooled slowly to room temperature. $AgNO_3$ solutions of different concentrations were prepared, and then 15 μL of the different concentrations $AgNO_3$ solutions were mixed with 35 μL DNA immobilization buffer containing 500 nM presulfided DNA strands, and the resulting solution maintained for 30 min at 37 °C, leading to the formation of Ag^+-packaged hairpin DNA. The SiO_2 dispersion was then activated by addition of 5 μL of 0.1 M PBS (containing 0.5 mg/mL EDC and 0.5 mg/mL NHS, pH 7.4) for 0.5 h, and then mixed with the Ag^+-packaged hairpin DNA solution. The resulting dispersion was then held at 37 °C for 30 min. Subsequently, 5 μL of 0.1 mg/mL avidin was added and the dispersion maintained for 60 min at 37 °C, obtaining Avidin-SiO_2-hDNA@Ag. In addtion, single stranded (ssDNA) without treatment with Ag^+ was directly assembled onto SiO_2 surface, obtaing SiO_2-ssDNA. After incubation with avidin, the Avidin-SiO_2-ssDNA bioconjugates were prepared.

2.3 PEC biosensor fabrication and PEC detection

Before preparing the PEC sensing interfaces, the ITO conductive glass substrates (5×1 cm^2) were thoroughly cleaned ultrasonically in an ethanol/NaOH mixed solution (v/v, 1:1) for 30 min, then acetone for 30 min and finally doubly distilled deionized water for 30 min. This process was followed by drying at 60 ^oC for 2 h. After cooling to room temperature, 40 μL the 1 mg/mL $BiVO_4$@TiO_2 dispersion was carefully dropped onto the bare ITO glass and dried under an infrared lamp. The obtained

electrode was denoted herein as $BiVO_4$@TiO_2/ITO. Then, 40 μL the MoS_2-Au NPs nanohybrid dispersion was carefully dropped onto the $BiVO_4$@TiO_2/ITO electrode surface and dried under an infrared lamp irradiation. The resulting electrode (denoted MoS_2-Au/$BiVO_4$@TiO_2/ITO) was then incubated with 20 μL of 10 M PBS containing 10 μg/mL anti-m^6A antibody for 2 h at 37 ^oC in a humidified chamber. The anti-m^6A antibody was captured onto the electrode surface, through the Au-S bond between -SH of antibody and AuNPs. The obtained electrode was denoted Ab/MoS_2-Au/$BiVO_4$@TiO_2/ITO and rinsed with washing buffer three times. Subsequently, 20 μL TE buffer (10 mM Tris–HCl,1 mM EDTA, pH 8.0, pH 7.4) containing different concentrations of m^6ATP was added onto the Ab/MoS_2-Au/$BiVO_4$@TiO_2/ITO surface, and the electrode was kept at 37 °C for 60 min in a humid environment. The electrode was then rinsed with washing buffer for three times, and named as m^6ATP/Ab/MoS_2-Au/$BiVO_4$@TiO_2/ITO. Afterwards, 20 μL Phos-tag-biotin reaction buffer containing 10 μM Phos-tag-biotin carefully dropped on the modified electrode surface, followed by incubation at 37 °C for 60 min. After rinsing with washing buffer for three times, Phos-tag/m^6ATP/Ab/MoS_2-Au/$BiVO_4$@TiO_2/ITO was obtained. This electrode was then incubated with 40 μL of the Avidin-SiO_2-hDNA@Ag dispersion for 60 min at 37 °C, followed by rinsing three times with washing buffer. The prepared electrode was denoted as hDNA@Ag/Phos-tag/m^6ATP/Ab/MoS_2-Au/$BiVO_4$@TiO_2/ITO. Subsequently, 10 μL DNA hybridization buffer containing 1 mM complementary DNA was mixed with 10 μL of 100 μg/mL Avidin-HRP and maintained for 60 min at

37 ^{o}C. This mixture of Avidin-HRP and DNA was then carefully dripped onto the surface of the hDNA@Ag/Phos-tag/m^{6}ATP/Ab/MoS_2-Au/$BiVO_4$@TiO_2/ITO electrode and incubated for 2 h at 37 ^{o}C in a humidified chamber, obtaining HRP-dsDNA/Phos-tag/m^{6}ATP/Ab/MoS_2-Au/$BiVO_4$@TiO_2/ITO. Besides, the Phos-tag/m^{6}ATP/Ab/MoS_2-Au/$BiVO_4$@TiO_2/ITO electrode was treated successively with 20 μL HRP-Avidin-SiO_2-ssDNA and the reaction mixture of Avidin-HRP and DNA, the obtained electrode was named as HRP-dsDNA/Phos-tag/m^{6}ATP/Ab/MoS_2-Au/$BiVO_4$@TiO_2/ITO1.

For PEC detection, 10 mM PBS (pH 7.4) containing different concentrations of H_2O_2 were used as the detection solution. The HRP-dsDNA/Phos-tag/m^{6}ATP/Ab/MoS_2-Au/$BiVO_4$@TiO_2/ITO electrode was used as working electrode and PEC response was recorded in the above solutions under visible light irradiation.

2.4 Sample preparation

Mature seeds of maize were obtained from College of Life Science, Beijing Normal University. These seeds were divided equally into control and experimental groups, and implanted in a few small pieces of gauze in a petri dish. After that, the control and experimental groups were soaked with redistilled deionized water and EMS diluent respectively for several days at normal temperature for germination. Subsequently, these seedlings were further cultured for seven days and the leaves were picked, and then the total RNA was extracted.

Chicken fetal hepatocytes were obtained from the liver of 15-day-old chicken and

cultured according to method previously (Cai et al. 2011). The cells were plated at a density of 1 x $l0^5$ – 1 x 10^6 cells/mL and kept in a humid atmosphere containing 5% CO_2. After the attachment of fetal hepatocytes on the culture plates, the pre-cultured fetal hepatocytes were exposed to one of the following treatments, the basal serum-free medium and the basal medium with different concentration insulin (0, 50, 100 and 200 nM). This process was maintained for 24 h, and then the cells were collected and the total RNA was isolated.

3. Results and discussion

Scheme 1.

3.1. Experiment principle

In this work, we developed a novel PEC method for the assay of m^6A based on $BiVO_4@TiO_2$ heterojunction and MoS_2-AuNPs photoactive materials, immunoreaction between m^6ATP and m^6A antibody, and an ingenious transfer of silver from C-Ag^+-C to the MoS_2-AuNPs system triggered by HRP catalyzed H_2O_2 reduction, culminating in the Ag deposition onto surface of the AuNPs.

Scheme 1 describes the different stages in the construction of the PEC biosensor and the mechanism of detection. $BiVO_4@TiO_2$ heterojunctions were first coated on the bare ITO electrode, followed by the MoS_2-AuNPs. It should be noted that the AuNPs served three functions in this biosensor: (1) they act as visible light absorbers, leading to the injection of hot electrons into the conduction band of MoS_2; (2) they serve as carriers to immobilize m^6A antibody by Au-S bond between AuNPs and –SH

of antibody; and (3) they are the site of Ag^+ adsorption and reduction. After addition of the MoS_2-AuNPs, m^6A antibody was then adsorbed on the electrode surface. m^6ATP was then introduced through immunoreaction between antigen (m^6ATP) and antibody (anti-m^6A antibody). Subsequently, biotin functionalized Phos-tag (Phos-tag-biotin) was added through specific interaction between Phos-tag and phosphate group of the ribonucleotide, and served as the link-bridge. Avidin-SiO_2-hDNA@Ag bioconjugates were then loaded onto the electrode surface. Finally, after hybridization with complementary DNA, Ag^+-packaged hairpin DNA was unfolded, resulting in the release of Ag^+ and the introduction of HRP. Due to the catalytic activity of HRP towards H_2O_2, O_2^- was generated in situ and served as an electron donor in solution with the pH value of 7.4, inducing the reduction of Ag^+ to Ag^0 on the AuNPs surface, producing a strong PEC response. With increasing m^6ATP concentration, more Avidin-SiO_2-hDNA@Ag bioconjugates were immobilized and more Ag^0 was deposited on the Au NPs, resulting in a stronger photocurrent. Hence, photocurrent intensity could be correlated with m^6A concentration.

3.2 Characterization of $BiVO_4$@TiO_2 heterojunctions, MoS_2-Au NPs

Fig. 1

The morphologies and structure of the as-prepared $BiVO_4$@TiO_2 heterojunctions were characterized by SEM and X-ray diffraction (XRD), respectively. Fig. 1A confirms the successful deposition of TiO_2 on the surface of the $BiVO_4$. The XRD pattern of the $BiVO_4$ product is shown in Fig. 1B. The data confirms the successful synthesis of monoclinic $BiVO_4$, evidenced by the characteristic peaks at $2\theta = 18.67°$

and 18.99° due to {110} reflections and the intense peak at 30.55° due to {010} reflection (curve a). Deposition of TiO_2 to form the $BiVO_4$@TiO_2 heterojunctions did not alter the crystal phase and crystallinity of the $BiVO_4$ (Fig. 1B, curve b). No XRD peaks belonging to TiO_2 were detected (note: the most intense XRD peaks for anatase and rutile polymorphs of TiO_2 are the (Grosjean) and {110} reflections, typically observed at $2\theta = 25.3^o$ and 27.45^o, respectively). It could be attributed to 1) the low weight percentage of TiO_2 in the heterojunction structure and 2) the lower crystallinity of the TiO_2 relative to the highly crystalline $BiVO_4$. As displayed in Fig. 1C, MoS_2 presents a characteristic sheet structure. Fig. 1D exhibits the successful preparation of MoS_2-AuNPs with 10-100 nm sized AuNPs decorating the MoS_2 surface.

3.3. Characterization of the immunosensor

Fig. 2

Electrochemical impedance spectroscopy (EIS) was a very powerful and useful tool for following the stepwise fabrication of the biosensor. The self-assembly process of the PEC biosensor was characterized by electrochemical impedance spectroscopy (EIS) in 5 mM $Fe(CN)_6^{3-/4-}$ (1:1) solution. As shown in Fig. 2A, the Nyquist plot of the bare ITO electrode displayed a small semicircle with an interface electron transfer impedance (R_{et}) value about 40 Ω (curve a). After the $BiVO_4$@TiO_2 heterojunctions were coated on ITO electrode, the semicircle increased in diameter (curve b), indicating that the immobilized $BiVO_4$@TiO_2 hindered the diffusion efficiency of the redox probe to the electrode. The R_{et} decreased slightly when MoS_2-AuNPs nanohybrids were deposited onto the $BiVO_4$@TiO_2/ITO electrode (curve c),

confirming the acceleration of electron transfer by MoS_2-AuNPs. As expected, the R_{et} value increased significantly when the m^6A antibody was immobilized on the electrode surface (curve d). The diffusion of the redox probe was clearly hindered by the large volume of the antibody. After the immobilization of m^6ATP, the R_{et} value was again increased (curve e), which is either a size effect or an electrostatic repulsion effect caused by the introduction of the phosphate group with two negative charges. These negative charges could repel $Fe(CN)_6^{3-/4-}$ probe away from the electrode surface. Due to the insulating effect of biomolecule, the R_{et} increased significantly when the Phos-tag-biotin was successfully captured by the phosphate group of m^6ATP (curve f). Subsequently, Avidin-SiO_2-hDNA@Ag bioconjugates were specifically incorporated onto the Phos-tag/m^6ATP/Ab/MoS_2-Au/$BiVO_4$@TiO_2/ITO electrode resulting in a further increase of R_{et} (curve g). This could be explained by two factors: (1) the electrostatic repulsion of $Fe(CN)_6^{3-/4-}$ by the negatively charged phosphate backbone of the oligonucleotides; or (2) a steric hindrance effect impairing the ability of the redox probe to transfer an electron to electrode surface. Finally, after the hybridization reaction, the R_{et} value showed an obvious increase (curve h), owing to 1) the electrostatic repulsion between the negatively sugar phosphoric acid backbone of complementary DNA and $Fe(CN)_6^{3-/4-}$ and 2) the insulating properties of the HRP biomolecule. Based on the above results, the successfully fabrication of the biosensor can be confirmed.

3.4. Detection feasibility assay

To confirm the detection feasibility of the biosensor, photocurrents of the ITO

electrode following different modifications were recorded in 0.1 M PBS containing 200 nM H_2O_2 under visible light irradiation. As shown in Fig. 2B, after deposition of $BiVO_4$@TiO_2 heterojunction (curve a) or MoS_2-AuNPs (curve b) on the ITO slide, weak photocurrents were obtained. After MoS_2-AuNPs was coated onto the $BiVO_4$@TiO_2/ITO electrode, the PEC response of the resulting MoS_2-Au/$BiVO_4$@TiO_2/ITO electrode increased (curve c). MoS_2-Au as a photoactive material therefore enhanced the photocurrent of $BiVO_4$@TiO_2. However, the obtained photocurrent was still weak, which was rationalized by the absence of an electron donor. A stronger photocurrent was observed for HRP-dsDNA@Ag/Phos-tag/m^6ATP/Ab/MoS_2-Au/$BiVO_4$@TiO_2/ITO electrode (curve d). It could be explained that in the presence of HRP, H_2O_2 was hydrolyzed to produce the electron donor O_2^-, which therefore caused in the observed increase of the photocurrent. To further verify the importance of Ag deposition on the AuNPs to the measured photocurrent, Avidin-SiO_2-ssDNA was prepared without Ag^+ and grafted onto the Phos-tag/m^6ATP/Ab/MoS_2-Au/$BiVO_4$@TiO_2/ITO electrode surface. The photocurrent of HRP-dsDNA/Phos-tag/m^6ATP/Ab/MoS_2-Au/$BiVO_4$@TiO_2/ITO1 electrode decreased (curve e). Based on the experimental PEC responses, it can be concluded that the HRP-dsDNA@Ag/Phos-tag/m^6ATP/Ab/MoS_2-Au/$BiVO_4$@TiO_2/ITO electrode developed here is suitable for the PEC detection of m^6A.

3.5. Optimization of detection conditions

See supplementary material.

Fig. 3

3.6. Analytical performance

Fig. 4

Under the optimal experiment conditions, the quantitative detection of m^6A was achieved. Fig. 4A shows the relationship between the PEC response and m^6ATP concentration. The PEC response increased with m^6ATP concentration in the range of 0.005 to 10 nM, and then remained almost constant at higher concentrations. Fig. 4B shows the PEC response plotted against the logarithm of the m^6ATP concentration in the concentration range 0.005 to 10 nM. A good linear relationship was established, an described by the equation of I (μA) = 0.51 log$c$(nM) + 1.79 (R=0.9989). The detection limit (LOD) was calculated to be 1.665 pM (S/N=3). In our previous work, m^6A was detected with the detection limit of 3.53 pM (Wang et al. 2017a). Lin et al. developed a electrochemiluminescence sensor for m^6A assay with a detection limit of 0.77 nM (Lin et al. 2010). Thus, compared with these prior reports, the PEC biosensor developed in this work affords a much lower m^6A detection limit.

The selectivity of the proposed method was assessed by using two different interferents, ATP and dATP. The Ab/MoS_2-Au/$BiOV_4$@TiO_2/ITO electrodes were incubated with different interferents (20 μL, 10 nM), respectively and then further incubated with Phos-tag-biotin, Avidin-SiO_2-hDNA@Ag and complementary DNA with HRP successively, as described in section 2.3. The PEC response was recorded and noted as I_1. And the change of the photocurrent ($\Delta I=I_1-I_0$) was compared, where I_0 represented the photocurrent of Ab/MoS_2-Au/$BiOV_4$@TiO_2/ITO electrode. As can

been seen from Fig. 4C, the ΔI of Ab/MoS_2-Au/$BiOV_4$@TiO_2/ITO incubated with ATP and dATP were lower than that with interferents, indicating that the above biomolecules could not be recognized anti-m^6A antibody, resulting in the failure following modification processes. Accordingly, the PEC biosensor showed a remarkable specificity for m^6A.

The reproducibility of the PEC biosensor was estimated by the variation coefficients of PEC response for seven independently fabricated biosensors. As shown in Fig. 4D, a relative standard deviation (RSD) of 4.36% was obtained across the seven biosensors, suggesting acceptable reproducibility in fabrication and performance.

3.7. Analysis of Real Samples

Fig. 5

In order to further explore the practicality of the PEC biosensor, it was applied to investigate the expression content change of m^6A in total RNA extracted from the leaves of maize seedlings and chicken fetal hepatocyte, where the two kinds of samples were treated with EMS (chemical mutagen) and insulin (hormone), respectively. In order to acquire and detect the expression level change of m^6A, the total RNA was first extracted from leaves and cells by Trizol, and the concentrations quantified by UV-Vis Q5000 micro volume spectrophotometry (USA). The RNA samples were diluted to the same concentration and then incubated with 100 μg/mL RNase A for 2 h at 37 °C. Afterwards, the total RNA and the digested solution were analyzed by agarose gel electrophoresis. As depicted in Fig. 5A, the expression levels

of m^6A in normal maize bud (column a) were lower than that in the EMS mutagenesis maize leaves (column b), indicating that EMS mutagenesis increased the expression of m^6A. As presented as Fig. 5B, the content of m^6A in chicken fetal hepatocyte increased with increasing insulin concentration from 50 to 200 nM. This experimental data states that insulin could also accelerate the expression of RNA methylation in chicken fetal hepatocyte. Based on the above investigation, one can conclude that the developed method could be used to detect the level of m^6A in complex biological samples.

4. Conclusions

In summary, a dual-signal amplification PEC bioanalysis was successfully developed for m^6A detection based on $BiVO_4@TiO_2$ heterojunction photoactive material, O_2^- generated by horseradish peroxidase conjugated biotin as electron donor, and an ingenious transfer of Ag from C-Ag^+-C to MoS_2-AuNPs. The PEC biosensor showed excellent detection selectivity and sensitivity, with detection limit of 1.665 pM. In addition, the PEC biosensor was successfully used for the assay of the expression level change of m^6A methylated RNA in maize bud and chicken hepatocyte, respectively. Results suggested that PEC biosensor may be useful for monitoring the regulation function of RNA methylation in eukaryotes.

Acknowledgements

This work was supported by the Natural Science Foundation of Shandong province China (Nos. ZR2016BM10), the National Natural Science Foundation of China (No. 21375079, 21775090), Founds of Shandong “Double Tops” Program

(SYL2017XTTD15) and the Taishan Scholars Program (No.201511023).

References

Albers, R.J., Coffin, B., Rottman, F.M., 1981. Anal. Biochem. 113, 118-123.

Baek, S.-W., Park, G., Noh, J., Cho, C., Lee, C.-H., Seo, M.-K., Song, H., Lee, J.-Y., 2014. ACS nano 8, 3302-3312.

Cai, Y., Song, Z., Wang, X., Jiao, H., Lin, H., 2011. Stress 14, 273-281.

Du, X., Dai, L., Jiang, D., Li, H., Hao, N., You, T., Mao, H., Wang, K., 2017. Biosens. Bioelectron. 91, 706-713.

Dubin, D.T., Taylor, R.H., 1975. Nucleic Acids Res. 2, 1653-1668.

Enkin, N., Sharon, E., Golub, E., Willner, I., 2014. Nano Lett.14, 4918-4922.

Fustin, J.-M., Doi, M., Yamaguchi, Y., Hida, H., Nishimura, S., Yoshida, M., Isagawa, T., Morioka, M.S., Kakeya, H., Manabe, I., 2013. Cell 155, 793-806.

Feng, J., Li, Y., Gao, Z., Lv, H., Zhang, X., Fan, D., Wei, Q. 2017. Biosens. Bioelectron. 99, 14-20.

Grosjean, H., Droogmans, L., Roovers, M., Keith, G., 2007. Method. Enzymol. 425, 55-101.

He, C., 2010. Nat. Chem. Biol. 6, 863-865.

Huang, X., Zeng, Z., Bao, S., Wang, M., Qi, X., Fan, Z., Zhang, H., 2013. Nat. Commun. 4, 1444.

Kane, S.E., Beemon, K., 1985. Mol. Cell. Biol. 5, 2298-2306.

Kellner, S., Burhenne, J., Helm, M., 2010. RNA Biol. 7, 237-247.

Kudo, A., Omori, K., Kato, H., 1999. J Am. Chem. Soc. 121, 11459-11467.

Li, C., Wang, S., Wang, T., Wei, Y., Zhang, P., Gong, J., 2014. Small 10, 2783-2790.

Li, H., Yu, H., Quan, X., Chen, S., Zhao, H., 2015a. Adv. Funct. Mater. 25, 3074-3080.

Li, H., Yu, K., Lei, X., Guo, B., Fu, H., Zhu, Z., 2015b. J Phys. Chem. C 119, 22681-22689.

Li, X., Zhu, L., Zhou, Y., Yin, H., Ai, S., 2017. Anal. Chem. 89, 2369-2376.

Liebich, H., Müller-Hagedorn, S., Klaus, F., Meziane, K., Kim, K.-R., J Chromatogr. A 1071, 271-275.

Lin, Z., Wang, W., Jiang, Y., Qiu, B., Chen, G., 2010. Electrochim. Acta 56, 644-648.

Ono, A., Cao, S., Togashi, H., Tashiro, M., Fujimoto, T., Machinami, T., Oda, S., Miyake, Y., Okamoto, I., Tanaka, Y., 2008. Chem. Commun. 39, 4825-4827.

Singh, A.P., Kodan, N., Mehta, B.R., Held, A., Mayrhofer, L., Moseler, M., 2016. ACS Catal. 6, 5311-5318.

Swasey, S.M., Leal, L.E., Lopez-Acevedo, O., Pavlovich, J., Gwinn, E.G., 2015. Sci. Rep. 5, 10163-10171.

Tateno, H., Miseki, Y., Sayama, K., 2017. Chem. Commun. 53, 4378-4381.

Wang, H., Zhang, Q., Yin, H., Wang, M., Jiang, W., Ai, S., 2017a. Biosens. Bioelectron. 95, 124-130.

Wang, Z., Yan, Z., Wang, F., Cai, J., Guo, L., Su, J., Liu, Y., 2017b. Biosens. Bioelectron. 97, 107-114.

Xie, J., Zhang, H., Li, S., Wang, R., Sun, X., Zhou, M., Zhou, J., Lou, X.W.D., Xie, Y., 2013. Adv. Mater. 25, 5807-5813.

Yin, Z., Chen, B., Bosman, M., Cao, X., Chen, J., Zheng, B., Zhang, H., 2014. Small 10, 3537-3543.

Zang Y, L.J., Ju H., 2017, Biosens. Bioelectron. 96, 8-16.

Zhang, L., Dong, S., 2006. Anal. Chem. 78, 5119-5123.

Zhang, N., Zhang, L., Ruan, Y. F., Zhao, W. W., Xu, J. J., Chen, H. Y. 2017. Biosens. Bioelectron. 94, 207-218.

Zhang, Y., Shoaib, A., Li, J., Ji, M., Liu, J., Xu, M., Tong, B., Zhang, J., Wei, Q., 2016. Biosens. Bioelectron. 79, 866-873.

Zhao, W., Liu, Y., Wei, Z., Yang, S., He, H., Sun, C., 2016. Appl. Catal. B-Environ. 185, 242-252.

Zhu, C., Zeng, Z., Li, H., Li, F., Fan, C., Zhang, H., 2013. J. Am. Chem. Soc. 135, 5998-6001.

Figure captions

Scheme 1. Schematic representation of the PEC biosensor construction process for m^6A assay.

Fig. 1 (A) SEM image of $BiVO_4$@TiO_2 heterojunctions. (B) XRD patterns of $BiVO_4$ (a) and $BiVO_4$@TiO_2 heterojunctions (b). TEM image of MoS_2 (C) and MoS_2-AuNPs (D).

Fig. 2 (A) EIS of ITO (a), $BiVO_4$@TiO_2/ITO (b), MoS_2-Au/$BiVO_4$@TiO_2/ITO (c), Ab/MoS_2-Au/$BiVO_4$@TiO_2/ITO (d), m^6ATP/Ab/MoS_2-Au/$BiVO_4$@TiO_2/ITO (e), Phos-tag/m^6ATP/Ab/MoS_2-Au/$BiVO_4$@TiO_2/ITO (f), hDNA@Ag/Phos-tag/m^6ATP/Ab/MoS_2-Au/$BiVO_4$@TiO_2/ITO (g) and HRP/Phos-tag/m^6ATP/Ab/MoS_2-Au/$BiVO_4$@TiO_2/ITO (h) in 5 mM $K_3[Fe(CN)_6]/K_4[Fe(CN)_6]$ (1:1) containing 0.1 M KCl. (B) The photocurrent of different electrodes in 0.1 M PBS containing 200 nM H_2O_2. (a) $BiVO_4$@TiO_2/ITO, (b) MoS_2-Au/ITO, (c) MoS_2-Au/$BiVO_4$@TiO_2/ITO, (d) HRP-dsDNA/Phos-tag/m^6ATP/Ab/MoS_2-Au/$BiVO_4$@TiO_2/ITO, (e) HRP-dsDNA/Phos-tag/m^6ATP/Ab/MoS_2-Au/$BiVO_4$@TiO_2/ITO1.

Fig. 3 Effect of $BiVO_4$@TiO_2 (A), H_2O_2 (B), $AgNO_3$ (C) and m^6A antibody (D) concentration, immunoreaction time (E) and Avidin-SiO_2-hDNA@Ag immobilization time (F) on the PEC response of the biosensor.

Fig. 4 The PEC response of the biosensor with different m^6ATP concentrations: (a-h) 0.005, 0.05, 0.1, 1, 5, 10, 20, 30 nM. (B) The linear relationship between the photocurrent and the logarithm value of m^6ATP concentration in the range 0.005 to 10 nM. (C) Selectivity of the immunosensor for different targets: (a) 10 nM m^6ATP, (b) 10 nM ATP, (c) 10 nM dATP. (D) The PEC response of seven biosensors fabricated independently. The error bars in each plot represent the standard deviation of three measurements.

Fig. 5 The relative expression change of m^6A in maize seedling leaves (A) and chicken fetal hepatocyte (B). For A, b was treated with 0.7 % EMS, a was control. For B, a-d were treated with 0, 50, 100 and 200 nM insulin, respectively. The error bars represent the standard deviation of three parallel measurements of the same sample.

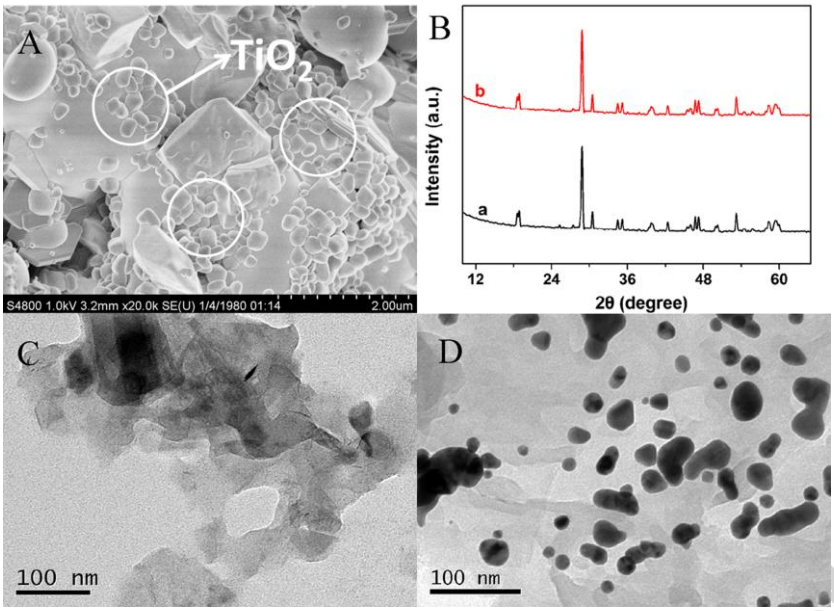

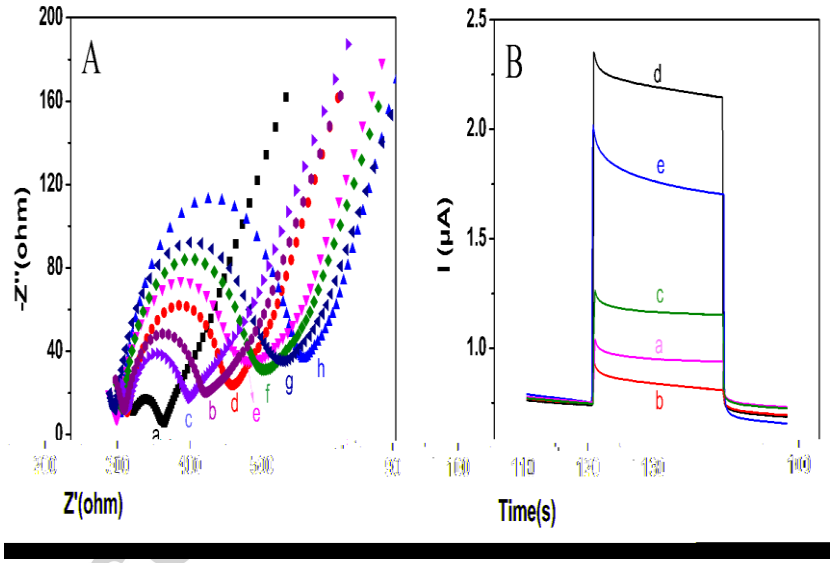

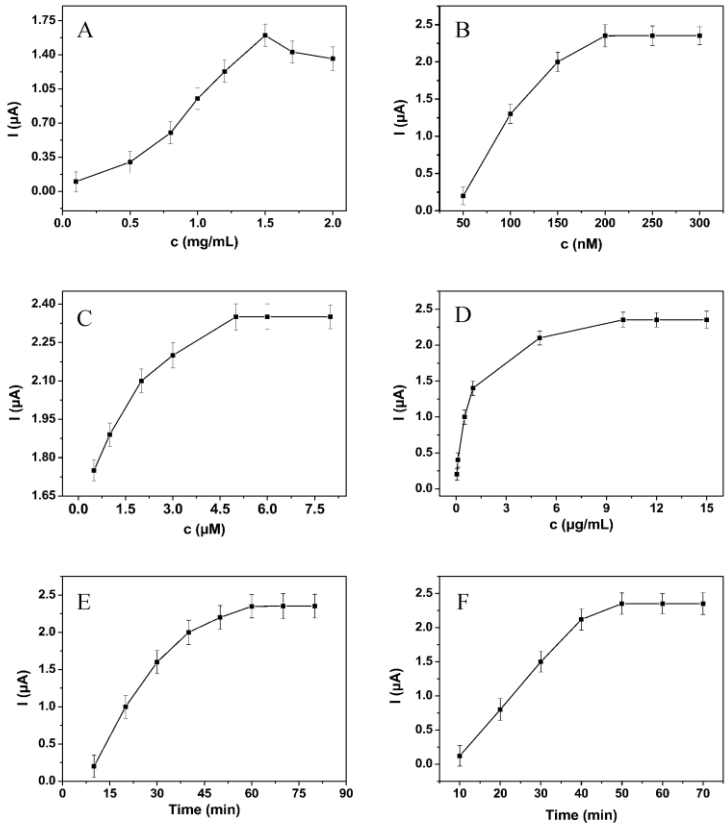
A
I (μA)
c (mg/mL)
B
I (μA)
c (nM)
C
I (μA)
c (μM)
D
I (μA)
c (μg/mL)
E
I (μA)
Time (min)
F
I (μA)
Time (min)

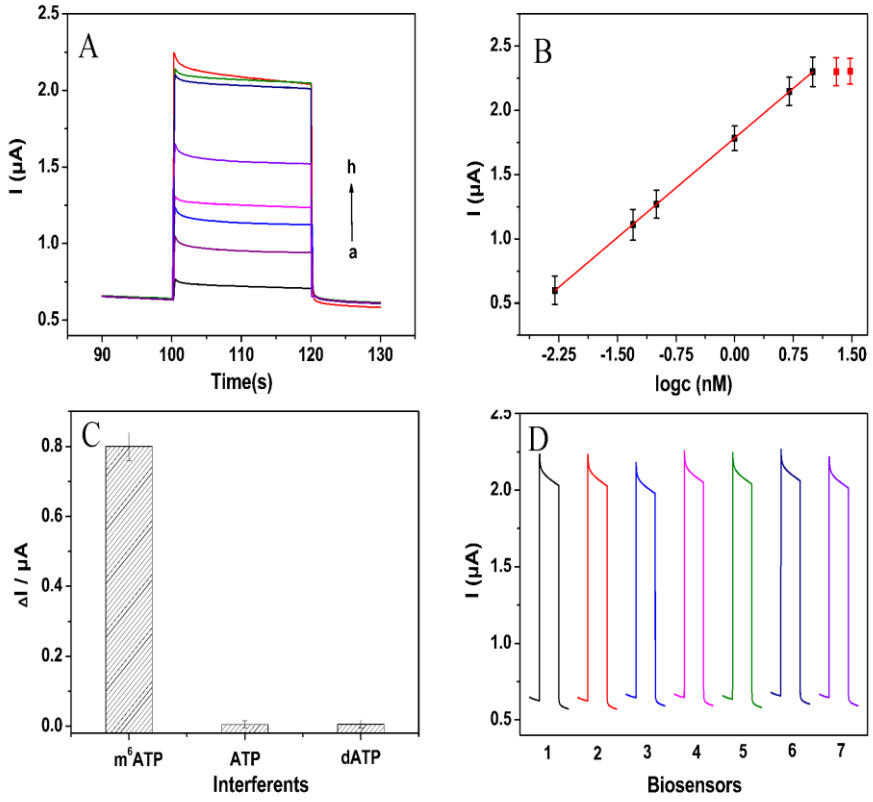
A
I (μA)
h
a
Time(s)
B
I (μA)
logc (nM)
C
ΔI / μA
m6ATP
ATP
dATP
Interferents
D
I (μA)
Biosensors

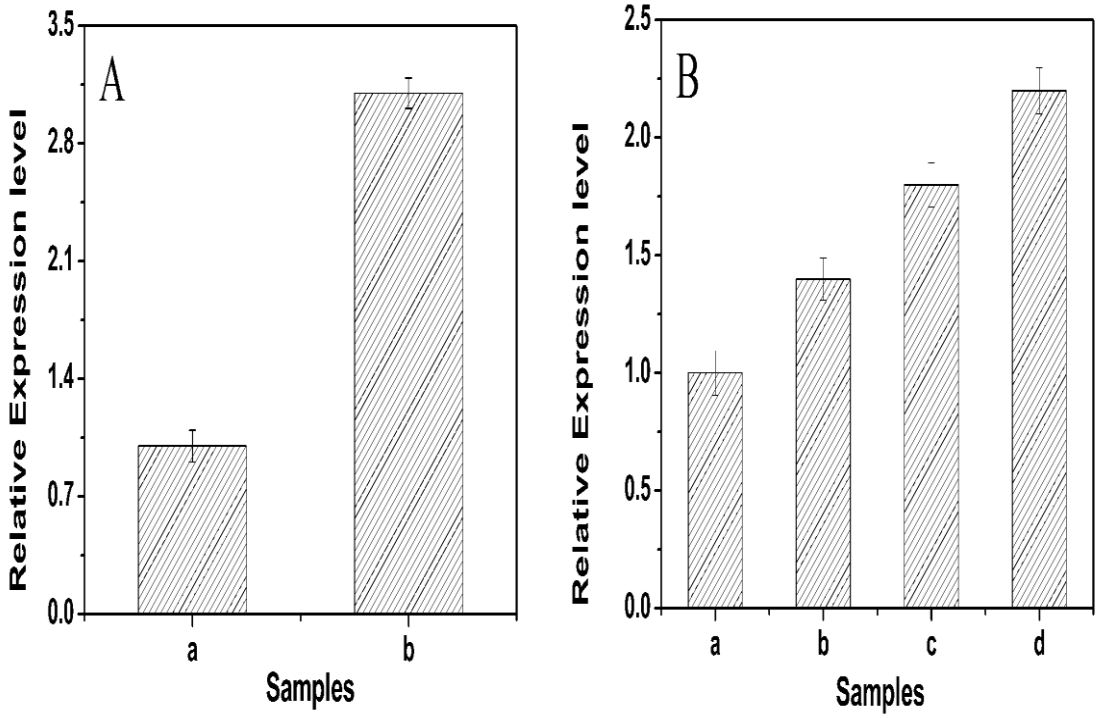
A
Relative Expression level
3.5
2.8
2.1
1.4
0.7
0.0
a
b
Samples
B
Relative Expression level
2.5
2.0
1.5
1.0
0.5
0.0
a
b
c
d
Samples

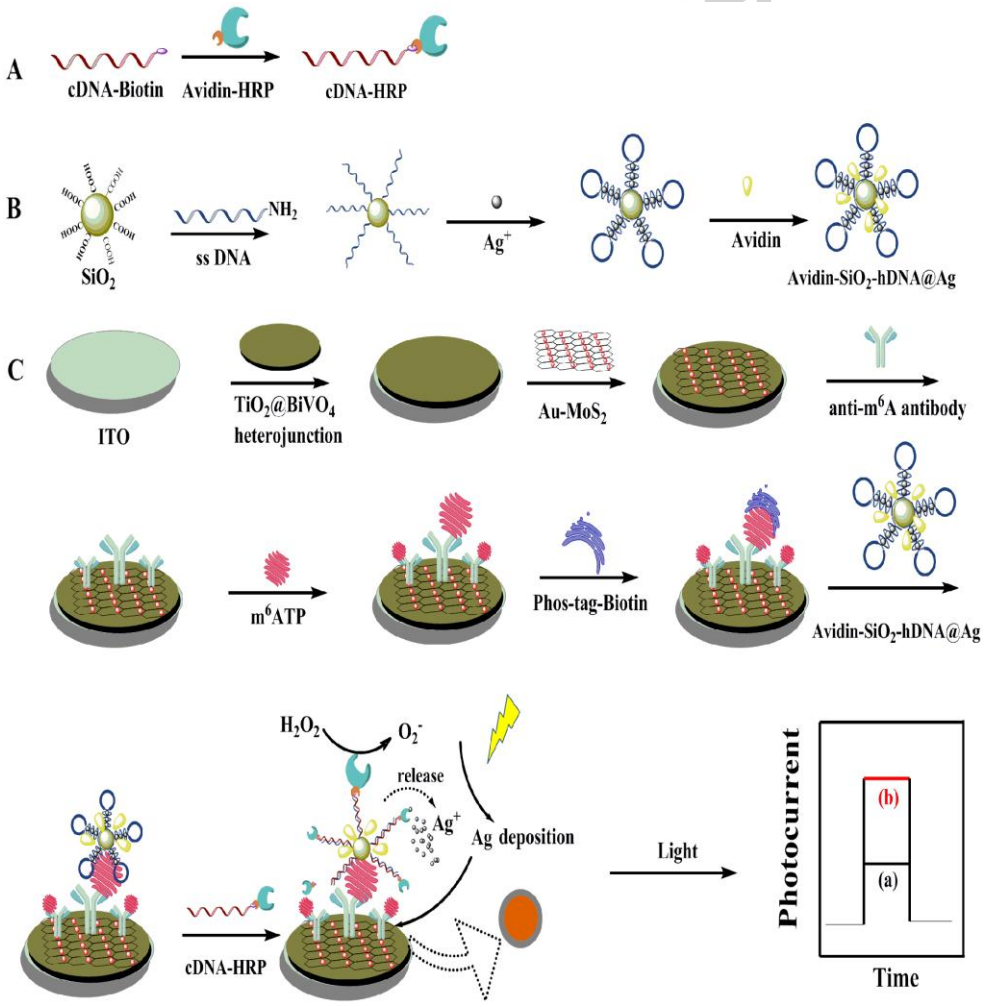
A
cDNA-Biotin
Avidin-HRP
cDNA-HRP
B
SiO2
NH2
ss DNA
Ag+
Avidin
Avidin-SiO2-hDNA@Ag
C
ITO
TiO2@BiVO4
heterojunction
Au-MoS2
anti-m6A antibody
m6ATP
Phos-tag-Biotin
Avidin-SiO2-hDNA@Ag
H2O2
O2-
release
Ag+
Ag deposition
cDNA-HRP
Light
Photocurrent
(b)
(a)
Time

Highlights

- A dual-signal amplified photoelectrochemical strategy was developed for N^6-methyladenosine detection.
- $BiVO_4$-110-TiO_2 heterojunction and gold nanoparticle decorated MoS_2 were used as photoactive materials.
- Ag^+-mediated cytosine pairs (C-Ag^+-C) was acted as the signal amplification unit.
- The photoelectrochemical biosensor was validated for detecting the change of m^6A content in the leaves of maize seedlings and chicken fetal hepatocyte.

Graphic Abstract